# LONG-TERM MONITORING OF DELIVERED LUMINOSITY AND CALIBRATION STABILITY IN THE CMS EXPERIMENT

O. Karacheban* on behalf the CMS Collaboration,
*CERN, Geneva, Switzerland*

*Abstract*

Over the course of the year different detector-specific effects can appear, e.g. temporary instability or efficiency loses. As the calibration of the luminosity detectors ("luminometers") is carried out only once per year, its long term stability monitoring is of crucial importance. The luminosity ratios measured by multiple luminometers as a function of time are used to identify regions of specific detector instability and to deliver the final luminosity uncertainty due to stability and linearity. Several times during the year so-called "$\mu$ scans" are performed to facilitate such detector comparisons over extended range of instantaneous luminosity. However, ratios between different detector measurements allow for measuring only relative nonlinearity, and new methods were required to measure nonlinearity for individual detectors and to derive the corrections to luminosity.From 2017 onwards CMS also explored the potential of "emittance scans", which were regularly performed and allowed for detector-independent stability and nonlinearity monitoring.Procedures used to measure the corrections and final luminosity uncertainty for 2018 data-taking period are reported.

## DETECTORS USED FOR LUMINOSITY

Multiple operational CMS online luminometers provided the benefit of uninterrupted and redundant luminosity measurement during LHC Run 2 (2015–2018).

The following detectors and algorithms are used for luminosity measurement: the Pixel Luminosity Telescope (PLT) [1, 2], with triple coincidence counting, the Forward Hadron calorimeter (HF) with occupancy algorithm and transverse energy sum algorithm (HFOC and HFET, respectively) [3], the pixel detector with pixel cluster counting (PCC) [4], and the Fast Beam Condition Monitor (BCM1F) composed of silicon (BCM1F Si) and polycrystalline diamond sensors (BCM1F pCVD) [2, 5] with hit counting. The luminosity is measured bunch by bunch, as a function of time and integrated over time. Measurement of one of these detectors with granularity of about 1.5 s and latency of about 1 s is sent online to CMS and LHC (so-called "best lumi"). The CMS pixel detector with pixel cluster counting (PCC) algorithm provides per bunch crossing measurement with latency of about 48 hours over a separate workflow. The PCC algorithm is used for offline lunimosity measurement. Also, part of the radiation monitoring system (RAMSES detectors) and drift tubes of the muon system (DT+RPC, hereafter DT) [3] are important complementary measurements for per-fill linearity and stability check of the integrated luminosity over the year. RAMSES and DT do not provide per-bunch luminosity are and are cross-calibrated to one of the online luminometers.

### *Data quality control*

Periods of instability of particular luminometer are excluded from the final luminosity data set.

The first stage of quality control is performed straight after each fill (offline fill validation), which is required to exclude pronounced instability of particular detector or periods of known detector interventions. The second stage of quality control takes place at the end of the year. It is based on the comparison of all detectors. In this analyses other problematic lumi-sections (LS), i.e., period of luminosity integrated over about 23 s, are identified and excluded.

## SPECIAL BEAM SCANS

Luminometers are calibrated using van der Meer (vdM) scans [6]. The vdM program is carried out once per year per collision mode. Wide beams, lower intensity than in the nominal LHC operation, and only solo bunches are used in vdM scans. Multiple corrections are applied to vdM scans to take into account known beam effects and the normalization uncertainty in the luminosity calibration is estimated, as described in detail in Refs. [3, 4, 7].

Special scans are required to measure the luminometer stability and linearity during the nominal LHC operation. During the year multiple filling schemes are used, bunches are grouped in trains, intensity is about 20% higher, pileup is about an order of magnitude larger than in vdM calibration fill, and collisions are performed with changing crossing angle and $\beta^*$.

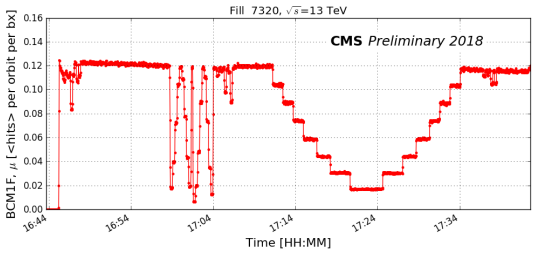


Figure 1: The hit rate reported by BCM1F pCVD during emittance scans in X and Y planes (17:00–17:05) and a $\mu$ scan (17:10–17:30). Three smaller drops in rate correspond to the LHC beam optimizations, which took place just at the beginning of stable beams, before and after the $\mu$ scan.

Per bunch crossing luminosity measurement is proven to be a powerful tool. Short vdM-like emittance scans showed

* olena.karacheban@cern.ch

a great potential [8, 9]. Example of such scans in X and in Y plane at the beginning of fill 7320 is shown in Fig. 1 (around 17:00–17:05). Similar to vdM scans, they allow for measuring the effective beam overlap and calculate the visible cross section ($\sigma_{\text{vis}}$) per luminometer per bunch crossing [9]. Emittance scans cannot be used to derive an absolute calibration, but open a wide range of possibilities for cross checks and have long lever arm across the fill.

One the one hand, effective beam overlap is a quantity of the beam and comparison of different detector measurements permit to spot individual detector effects. On the other hand, $\sigma_{\text{vis}}$ is a property of the detector and, assuming stable detector conditions, it is constant. Varying $\sigma_{\text{vis}}$ for different beam conditions points to nonlinearity of the detector and over time to change of the detector efficiency, respectively. Per-bunch current normalization to the total beam current and per-bunch correction for beam-beam deflections [10] are taken into account in the emittance scan analyses.

To measure relative nonlinearity simple detector ratios can be used. Several times per year $\mu$ scans [11] are performed. The $\mu$ scans are also special beam scans with extended per-step duration to increase the statistical power. As the primary purpose of $\mu$ scans is to probe a wide range of the instantaneous luminosity, they can be performed in multiple ways. $\mu$ scan in X and in Y plane are discussed in Ref. [11], but they can also be performed in one dimension. An example of one-dimension $\mu$ scan performed first reducing and then increasing the instantaneous luminosity is shown in Fig. 1 (17:10–17:35).

## EMITTANCE SCANS FOR STABILITY MONITORING

Regularly performed emittance scans provide access to relative change of the $\sigma_{\text{vis}}$ with respect to the absolute calibration carried out in a vdM program. Fig. 2 shows the efficiency of HFET algorithm in 2017 and 2018 pp data-taking period as a function of the integrated luminosity. The efficiency is defined considering $\sigma_{\text{vis}}$ from 2018 vdM scan (fill 6868) as a reference.

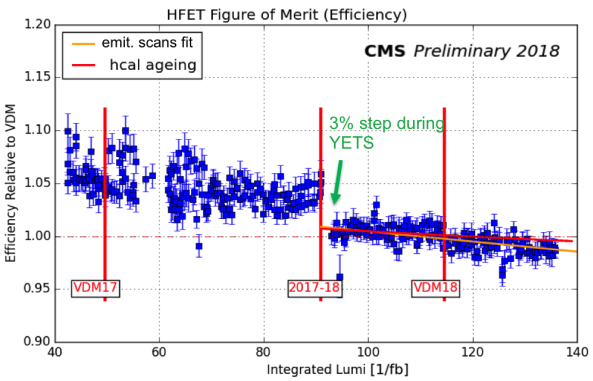


Figure 2: HFET algorithm efficiency in 2017–2018 defined from emittance scans with respect to the vdM calibration fill in 2018.

One point of the plot represents the emittance scan during one LHC fill, error bars cover the statistical spread over the bunches. It is seen that due to improved beam quality and more consistent filling scheme during operation in 2018 the spread between the points is minimized in relative to 2017, where the filling scheme was changed couple of times across the year. The 3% step-like change in the efficiency corresponds to the detector performance change after the extended year-end technical stop (YETS). The merit of emittance scans was that this change was noticed directly from the first days of the LHC operation. The observed slope is due to radiation damage of the detector, caused by the gain loss in the photomultiplier tubes and fibers in HF. The slope measured from the fit to emittance scan data (Fig. 2, orange) is slightly steeper than it was predicted in the HCAL aging model (Fig. 2, red). One slope value per year was defined and applied as efficiency correction to the whole data set. Similar analyses was done for HFOC.

For BCM1F pCVD and PLT due to detector interventions and optimization during the year, data were subdivided into the multiple regions for final efficiency correction. Fig. 3 shows BCM1F pCVD efficiency in 2018 proton-proton (pp) data-taking period. Different regions of detector efficiency are shown in different colors. Those regions are separated by technical stops, tests when the tracker was warmed up, or changes in detector settings, explaining the changes in the measured slope.

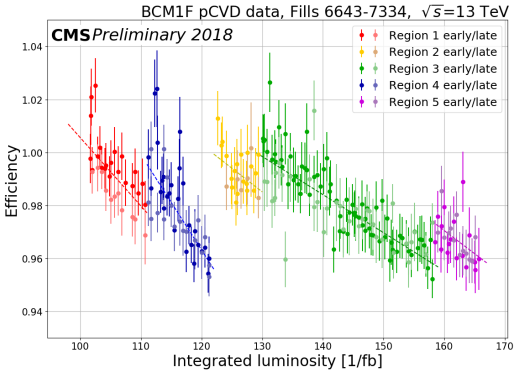


Figure 3: BCM1F pCVD efficiency in 2018 pp data-taking period defined from emittance scans with respect to 2018 vdM calibration fill.

## NONLINEARITY MEASUREMENTS USING EMITTANCE SCANS

In the long LHC fills a wide range of single bunch instantaneous luminosity (SBIL) is covered. At the beginning of the standard physics fill the SBIL from all bunches covers a range of 6–9 Hz/$\mu$b, when at the end of the fill it drops to 2–5 Hz/$\mu$b. Combining $\sigma_{\text{vis}}$ measurements in the emittance scans at the beginning ("early" scan) and at the end of the fill ("late" scan) detector nonlinearity is extracted. An example of $\sigma_{\text{vis}}$ as a function of SBIL is shown in Fig. 4 for leading

bunches in blue and train bunches in red. The slope of the fit to this data is a direct measurement of nonlinearity per unit of SBIL. Leading bunches are considered separately as they have different evolution of emittance in time and, therefore, show different linearity.

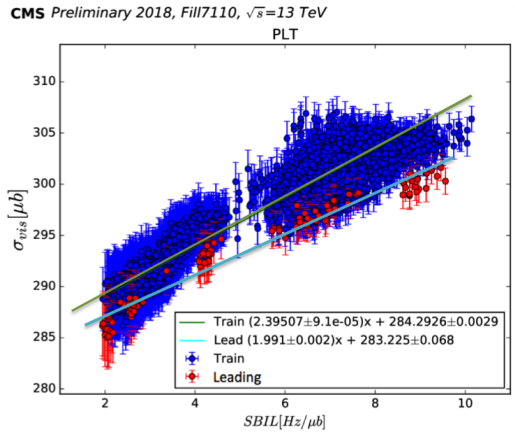


Figure 4: PLT $\sigma_{\text{vis}}$ as a function of single bunch instantaneous luminosity in Fill 7110 for leading and train bunches with first-order polynomial fits.

The advantage of this method is that it is a self-consistent check since no cross-detector comparisons are required, only single luminometer data is used. Measurements can be also performed per fill, when two emittance scans are available. Even measurement per scan can be considered. However, in Fig. 4 one can see that slope extracted for points only at low SBIL would be steeper than the one for high SBIL. This difference might be accounted for by the dynamic-$\beta$ correction [10], which had not been applied to emittance scans yet. The dynamic-$\beta$ correction is of higher importance, especially in the late emittance scans, as the size of the correction is a function of the bunch width, and spread of bunch width at the end of the fill is larger than at the beginning. Effort is ongoing in collaboration with beam dynamics experts.

Average nonlinearity measurements from several well separated in time fills for all CMS online luminometers for leading and train bunches are summarized in Table 1. The uncertainty corresponds to one standard deviation of the slopes measured in different fills.

## NONLINEARITY MEASUREMENTS USING $\mu$ SCANS

Based on the emittance scans analysis from different fills it was concluded that detector nonlinearity is stable during the year. Consequently, relative nonlinearity measured in multiple $\mu$ scan across the year for the same pair of detectors is expected to be compatible.

The advantage of $\mu$ scans over the emittance scans is independence from bunch current normalization and beam-beam effects, as they are similar for all detectors and, therefore, are canceled out in the luminosity ratios.

In 2018, $\mu$ scans were performed with solo bunches only (fill 6847), with 1200 colliding bunches with bunch trains (fill 6854), and in the standard physics fills with 2500 colliding bunches with bunch trains (fill 7320). Although data analysis is still ongoing, comparison of estimated slopes from $\mu$ scans analyses and emittance scans analyses are discussed. According to Ref. [11], the nonlinearity of BCM1F pCVD with respect to BCM1F Si averaged over all 1200 bunches in fill 6854 is -0.69 ± 0.18 (stat). This filling scheme is mainly composed of train bunches, and for final comparison leading and train bunches should be considered separately. Assuming from Table 1, that for train bunches BCM1F Si has almost zero nonlinearity within the error bars, agreement of $\mu$ scan and average nonlinearity measured from emittance scans agree very well. Relative slope of HFOC/BCM1F Si is reported to be 0.31 ± 0.14 (stat), it also agrees within error bars with results from Table 1 for HFOC train bunches. However, difference of the slope sign and size of the nonlinearity for HFET is to be investigated and understood, as from $\mu$ scan analysis negative relative slope of -0.09 ± 0.12 (stat) is reported.

Table 1: The nonlinearity of CMS online luminometers estimated from emittance scans. The mean of the slopes measured in the set of fills for leading and train bunched with uncertainty, corresponding to the standard deviation (STD) of the per-fill slopes.

| **Luminometer** | **nonlinearity (%/(Hz/μb))** | |
|---|---|---|
| | **Leading bunches** | **Train bunches** |
| HFET | 0.12 ± 0.09 | 0.27 ± 0.08 |
| HFOC | 0.03 ± 0.07 | 0.2 ± 0.07 |
| BCM1F pCVD | -0.67 ± 0.15 | -0.67 ± 0.11 |
| BCM1F Si | 0.35 ± 0.18 | 0.14 ± 0.12 |
| PLT | 1.03 ± 0.07 | 0.94 ± 0.08 |

Robust method of combining nonlinearity measured from two methods is to be established. For BCM1F pCVD also total rate dependency [5] has to be also taken into account. It means that slope measured is the fills with different number of bunches and different filling scheme will differ. Also bunch-dependent afterglow corrections have to be applied in each step of $\mu$ scan.

## FINAL LUMINOSITY UNCERTAINTY

Final comparisons of the luminosity ratios are done after corrections for known stability and nonlinearity effects described above are applied to each detector individually. It is important to note that all online detectors are individually calibrated and in the vdM fill integrated luminosity measured by HFOC, HFET, PCC, PLT, and BCM1F agree up to the level of 0.5% [3].

### *Final stability*

Figs. 5–6 show examples of luminometer pairs comparison [3]. Each data point corresponds to ratio of integrated over 50 LS (about 20 min of data) luminosity. Periods where

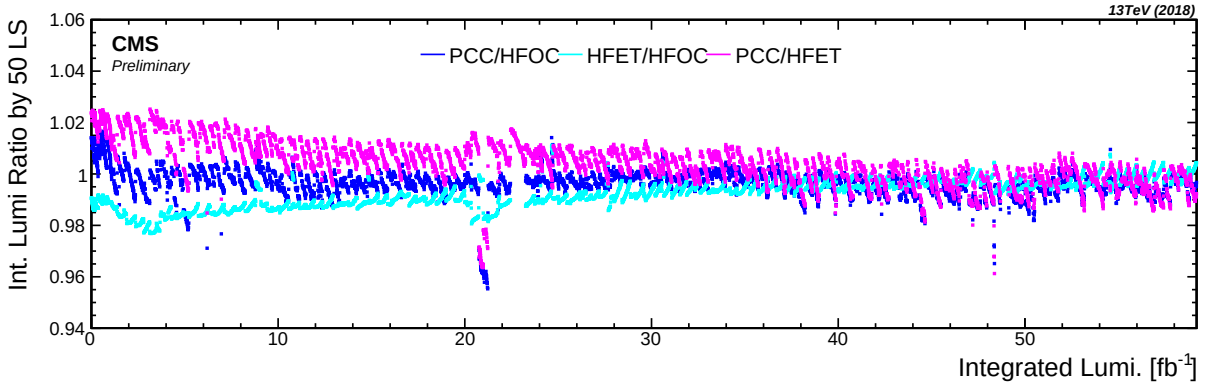


Figure 5: Stability comparisons for PCC, HFOC, and HFET across the 2018 data set [3].

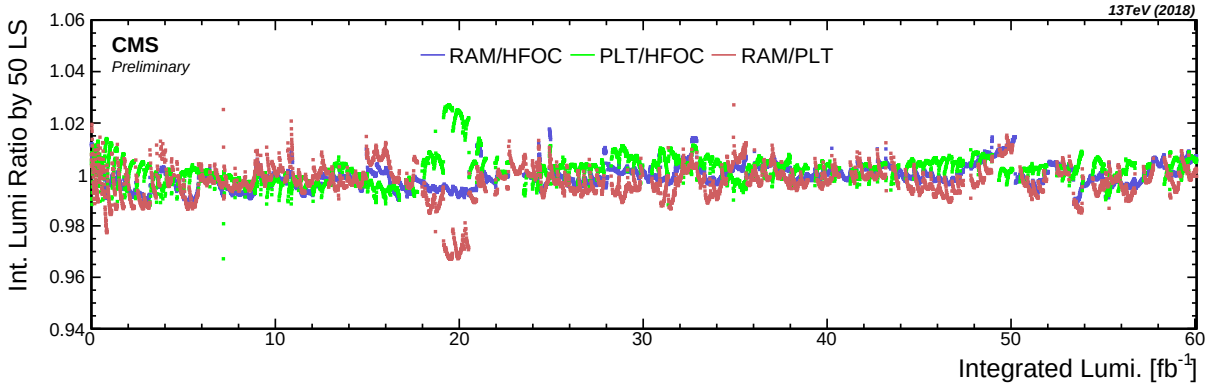


Figure 6: Stability comparisons for HFOC, RAMSES, and PLT across the 2018 data set [3].

an individual luminometer has known detector issues have been removed.

From all detector pairs, PCC/HFOC exhibit excellent stability over the course of the year. For PLT/HFOC, the overall stability is also good, only a small period of instability is seen for PLT at around 20 $fb^{-1}$ in Fig. 6, similar as it was seen for PCC in Fig. 5. One can conclude from ratios of three detectors which one is problematic, as a shift in the ratio away from unity is not seen for HFET/HFOC in Fig. 5 and in RAMSES/HFOC in Fig. 6.

To avoid frequent change of the luminosity source in the final physics data set, one luminometer which covers the majority of the per-year data is selected. The “best” luminometer with “second best" luminometer in the priority list cover 99% of the whole year data (in 2018 PCC and HFOC).

To evaluate the uncertainty due to stability, PCC/HFOC data in Fig. 5 is filled into a histogram weighted by the luminosity, as shown in Fig. 7. The standard deviation of this distribution is taken as the final luminosity uncertainty due to stability and amounts to 0.6%. Similar plots for all detector pairs are presented in Ref. [3]

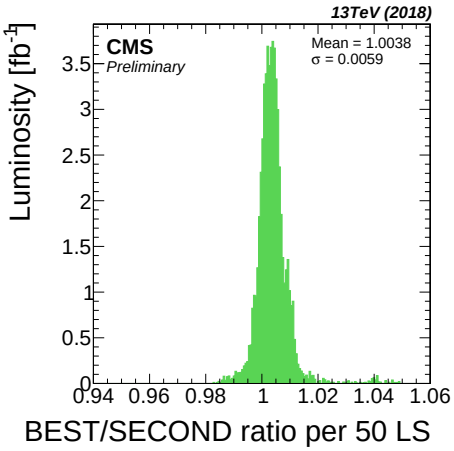


Figure 7: Histogram of luminosity ratio values between the best and second-best luminometer, weighted by luminosity. The standard deviation of the histogram is taken as the resulting systematic uncertainty [3].

### *Residual nonlinearity*

The linearity response of different luminometers is also compared to assign the systematic uncertainty in the linearity. This is done in two steps. First, for a given fill, the ratio of the luminosity values given by the two luminometers is plotted as a function of average SBIL. This ratio is then fitted with a first-order polynomial and the slope is taken as the relative nonlinearity for those two luminometers for that fill. Then, the extracted slope is plotted for different fills to monitor the consistency of measured nonlinearity. The results for the 2018 data are shown for PCC/HFOC in Fig. 8, and for different luminometer pairs are presented in Ref. [3].

The measured residual nonlinearity for PCC and HFOC (best and second best) with respect to each other is 0.2%/(Hz/$\mu$b). The nonlinearity is measured larger than that for HFOC, RAMSES, and BCM1F (Table 2), but it is conservatively applied to the overall 2018 luminosity. This results in the lumonisity uncertainty of 1.1% due to residual nonlinearity.

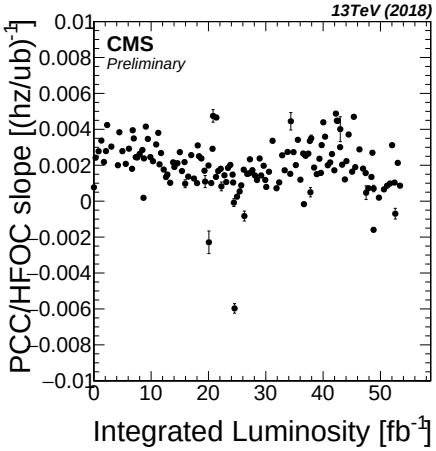


Figure 8: Results of the linearity studies for all 2018 fills for PCC and HFOC. Each point represents the slope of the first-order polynomial fit to luminosity ratios per fill as a function of integrated luminosity [3].

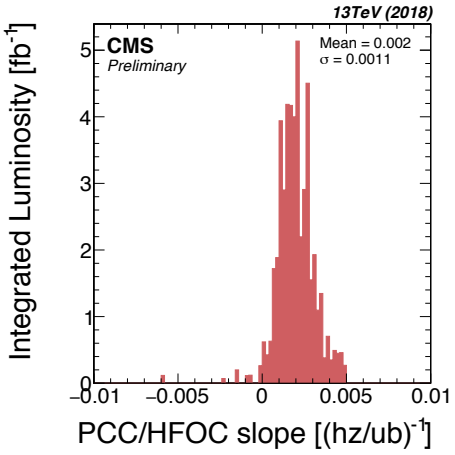


Figure 9: The slopes measured from the first-order polynomial fit to luminosity ratios PCC/HFOC per fill binned and weighted according to the luminosity in that fill [3]. Histogram of Fig. 8.

## CONCLUSION

the uncertainties due to cross-detector stability and linearity are reflect the detector operations over the course of the year and are based on our current understanding of the detector effects. In 2018, the uncertainty due to stability is 0.6% and due to residual nonlinearity is 1.1%. The availability of multiple luminometers is beneficial for estimating the associated corrections and the final luminosity uncertainty.

Table 2: Residual nonlinearity for each pair of CMS luminometers. The mean of the slopes between the two measurements, and the standard deviation (STD) of the per-fill slopes.

| **Luminometer pair** | **Residual nonlinearity (%/(Hz/$\mu$b))** | |
|---|---|---|
| | **Mean slope** | **STD slope** |
| PCC/HFET | 0.2 | 0.11 |
| PLT/HFOC | -0.07 | 0.17 |
| RAMSES/HFOC | 0.04 | 0.09 |
| DT/HFOC | 0.01 | 0.07 |
| BCM1F pCVD/ HFOC | -0.2 | 0.15 |
| HFET/HFOC | -0.09 | 0.07 |

The uncertainty due to nonlinearity is already one of the largest contributions and is expected to be only higher in Run 3 and HL-LHC. Therefore, improvements to currently used emittance scans and combination of methods, as e.g., $\mu$ scans and emittance scans are required. Understanding of the beam effects and all beam-related corrections will become essential for improvement of the precision of nonlinearity measured from emittance scans.

## ACKNOWLEDGMENT

The author would like to acknowledge colleagues from the CERN's Beams Department, in particular M. Hostettler, G. Trad and LHC operators for fruitful discussions and help to setup of the special runs. Many thanks to T. Pieloni and C. Tambasco (EPFL), I. Efthymiopoulos (BE-ABP-HSI), W. Kozanecki (ATLAS), and V. Balagura (LHCb) for the leading effort to improve the simulations and implement multiparticle approach to derive beam-beam corrections; M. Palm (BE-BI-PM) for his help to implement bunch current correction to first bunch in the train and derive ghost/satellite corrections.

## REFERENCES

[1] M. Barbero et al., Design and test of the CMS pixel readout chip, Nucl. Instrum. Methods Phys. Res., A 517 (2004) 349, DOI: 10.1016/j.nima.2003.09.043

[2] M. Guthoff on behalf of the CMS Collaboration, Instrumentation for beam radiation and luminosity measurement in the CMS experiment using novel detector technologies, Nucl. Instrum. Methods Phys. Res., Volume 845 (2017) 565, DOI: 10.1016/j.nima.2016.06.028

[3] CMS Collaboration, CMS luminosity measurement for the 2018 data-taking period at $\sqrt{s}$=13 TeV, CMS-PAS-LUM-18-002, `https://cds.cern.ch/record/2676164`

[4] CMS Collaboration, CMS luminosity measurement for the 2016 data-taking period, CMS-PAS-LUM-17-001, `https://cds.cern.ch/record/2257069`

[5] M. Guthoff on behalf of the CMS Collaboration, The new Fast Beam Condition Monitor using polycrystalline diamond sensors for luminosity measurement at CMS, ELBA2018,

Nucl. Instrum. Methods Phys. Res., A 936 (2019) 717, DOI: 10.1016/j.nima.2018.11.071

[6] S. van der Meer, Calibration of the Effective Beam Height in the ISR, CERN-ISR-PO-68-31 (1968)

[7] CMS Collaboration, CMS luminosity measurement for the 2017 data-taking period, CMS PAS LUM-17-004, https://cds.cern.ch/record/2621960

[8] M. Hostettler et al., Luminosity scans for beam diagnostics, Phys. Rev. Accel. Beams 21, (2018) 102801, DOI:10.1103/PhysRevAccelBeams.21.102801

[9] O. Karacheban, P. Tsrunchev on behalf of the CMS Collaboration, Emittance scans for CMS luminosity calibration, EPJ Web of Conferences 201 (2019) 04001, DOI: 10.1051/epjconf/201920104001

[10] A. Babaev on behalf of the CMS Collaboration, Beam-dynamic effects at the CMS BRIL van der Meer scans, JINST 13 (2018) C0302, DOI: 10.1088/1748-0221/13/03/C0302

[11] A. Babaev on behalf of the CMS Collaboration, Relative nonlinearity of BRIL luminometers derived from CMS $\mu$ scans , PoS (LHCP2019) 042